Inorg. Chem. **2008**, *47*, 6296−6302

High-Pressure Synthesis, Crystal and Electronic Structures, and Transport Properties of a Novel Perovskite $HgSnO_3$

Masashi Yoshida, Tetsuhiro Katsumata, and Yoshiyuki Inaguma*

Department of Chemistry, Faculty of Science, Gakushuin University, 1-5-1 Mejiro, Toshima-ku, Tokyo, 171-8588 Japan

Received February 27, 2008

We synthesized a novel perovskite-type oxide, $HgSnO_3$, under high pressure and high temperature, and investigated the crystal and electronic structures as well as the transport properties. It was found that $HgSnO_3$ possesses a trigonal-hexagonal lattice with space group $R\bar{3}c$. The band gap of $HgSnO_3$ estimated by diffuse reflectance spectrum measurement is relatively small (1.6 eV), irrespective of the large octahedral tilting distortion. The small band gap is caused by the increase in the bandwidth of the conduction and valence bands due to mixing between the empty Hg 6s orbitals and the antibonding Sn 5s-O 2p states and the mixing between the filled Hg 5d orbitals and the O 2p states, respectively. The electronic resistivity, Seebeck coefficient, and Hall coefficient measurements indicate that as-synthesized $HgSnO_3$ is an n-type semiconductor.

1. Introduction

Perovskite-type oxides, denoted by ABO_3, have attractive electronic properties that depend on both the kinds of elements at the A and B sites and the structure. In general, the network of a corner-shared BO_6 octahedral is in charge of these electronic functions, and the electronic structure can be indirectly controlled by whole or partial substitution of isovalent or allovalent ions for the A-site ion, which changes the crystal symmetry and brings in carrier doping.[1] However, the electronic orbital of the A-site ion in most of perovskite-type oxides does not directly participate in the electronic structure near the Fermi level.

Among the many studies of perovskite-type oxides, the crystal and electronic structures, as well as the relationship of stannate perovskites $ASnO_3$ (A = Ba, Sr, Ca, and Cd), have been well elucidated by Mizoguchi, Eng, and Woodward.[2] In stannate perovskites, the lowest-energy state in the conduction band primarily arises from the antibonding Sn 5s-O 2p interaction. In the alkaline-earth stannate perovskite $ASnO_3$ (A = Ba, Sr, and Ca), the conduction bandwidth strongly decreases with increases in the magnitude of the SnO_6 octahedral tilting distortion from $BaSnO_3$ to $CaSnO_3$. This change leads to a corresponding increase in the band gap from 3.1 eV in $BaSnO_3$ to 4.4 eV in $CaSnO_3$. In these compounds, electronic orbitals of alkaline-earth atoms do not directly contribute to the electronic structure near the Fermi level. In contrast, in $CdSnO_3$, the electronic orbitals of cadmium contribute to the electronic structure near the Fermi level. The band gap of $CdSnO_3$ is relatively small (3.0 eV), though the magnitude of the octahedral tilting distortion

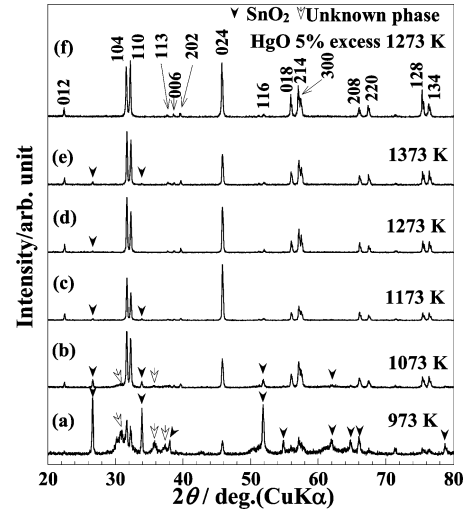

Figure 1. Powder X-ray diffraction patterns for the samples synthesized under 7 GPa for 30 min at various temperatures.

* To whom correspondence is addressed. E-mail: yoshiyuki.inaguma@gakushuin.ac.jp.

(1) (a) Mitchell, R. H. *Perovskites: Modern and Ancient*; Almaz Press Inc.: Thunder Bay, Ontario, Canada, 2002 (ISBN0−9689411−0-9). (b) Attfield, J. P. *Chem. Mater.* **1998**, *10*, 3239.

(2) Mizoguchi, H.; Eng, H. W.; Woodward, P. M. *Inorg. Chem.* **2004**, *43*, 1667.

10.1021/ic800370r CCC: $40.75
Published on Web 06/19/2008

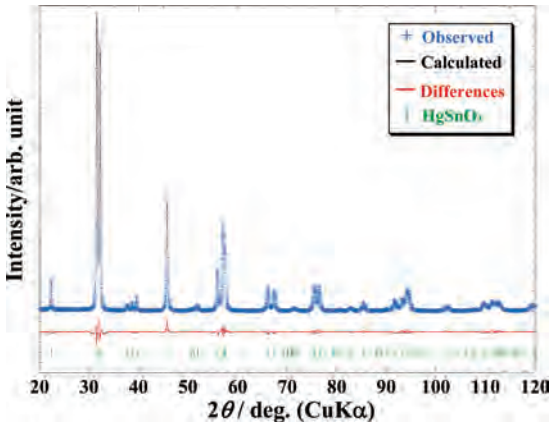

Figure 2. Rietveld refinement pattern of $HgSnO_3$. Plus (+) symbols represent the observed diffraction data, which are overlapped by a calculated pattern (solid line). Differences between observed and calculated intensities are plotted under the observed and the calculated pattern. The tick marks below the diffraction patterns denote the positions of possible Bragg reflections for $HgSnO_3$.

Table 1. Final Results of the Rietveld Refinement with the Powder X-ray Diffraction Data for $HgSnO_3$ [a]

atom	Site	*x*	*y*	*z*	*B*/Å^2
Hg	6*a*	0	0	1/4	0.60(5)
Sn	6*b*	0	0	0	0.38(5)
O	18*e*	0.3967(11)	0	1/4	1(fixed)

[a] Hexagonal, Space group: $R\bar{3}c$, $Z = 6$, $a = b = 5.551(3)$ Å, $c = 13.967(6)$ Å, $R_{wp} = 9.72\%$, $R_p = 6.87\%$, $S = 1.63$, $R_I = 1.35\%$, $R_F = 1.07\%$.

Table 2. Selected Interatomic Distance (Angstroms) and Bond Angle (Degrees) in $HgSnO_3$ and $CaSnO_3$[11]

bond	$HgSnO_3$	$CaSnO_3$[11]
Sn−O	2.0620(19)	2.061 × 2
		2.063
A−O	2.202(6) × 3	2.344
	2.8837(16) × 6	2.364 × 2
	3.349(6) × 3	2.414
		2.640 × 2
		2.792 × 2
		3.283
		3.406
		3.553 × 2
Sn−O−Sn	147.7(3)	146.6
		148.2

of $CdSnO_3$ is no smaller than that of $CaSnO_3$. The origin of this apparent small band gap is the mixing between the empty Cd 5s orbitals and the antibonding Sn 5s-O 2p states, resulting in the increase in the conduction bandwidth.[2]

Because mercury is a group 14 element, the same as cadmium, it is anticipated that the orbital of mercury contributes to the electronic structure in the vicinity of the band edge, the same as $CdSnO_3$. In this study, we therefore synthesized a novel perovskite, $HgSnO_3$, under high pressure and high temperature, and investigated the crystal and electronic structures as well as the transport properties. We discuss herein the participation of the mercury orbital in the electronic structure near the Fermi level.

2. Experimental Section

The perovskite-type oxide $HgSnO_3$ was synthesized by a solid-state reaction under high pressure. The starting materials were HgO (3N) and SnO_2 (3N). The stoichiometric or HgO 5 mol% excess mixture was sealed in a gold capsule (0.2 mm in thickness, 3.1 mm in inner diameter, and 3.2 mm in depth). A pyrophyllite cube block (13 mm in side length) was used as the pressure medium. A cylindrical graphite heater was place in the cube block. The capsule put in the NaCl sleeve was placed in the heater. NaCl disks were then stuffed at both ends of the heater. The mixture was allowed to react in a TRY cubic multianvil-type high-pressure apparatus (NAMO 2001) under a pressure of 7 GPa at 973 to 1373 K for 30 min and then was quenched down to room temperature. No weight loss was detected in the sample after the high pressure and heat treatment.

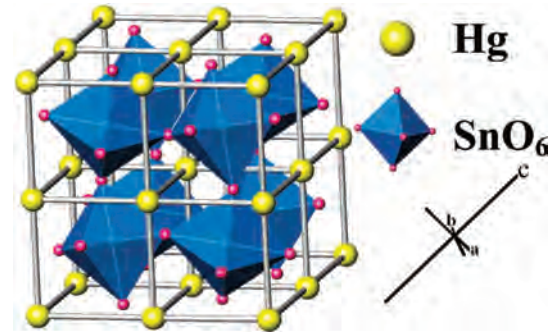

Figure 3. Crystal structure of $HgSnO_3$ from the perspective of the corner-shared SnO_6 octahedra framework.

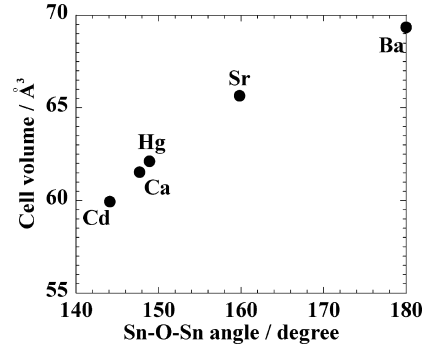

Figure 4. Primitive cell volume versus the average Sn−O−Sn angle of $ASnO_3$ (A = Hg, Cd, Ba, Sr and Ca).

Phase identification was carried out by the powder X-ray diffraction (XRD) method using a Rigaku RINT 2100 diffractometer (graphite monochromatized Cu Kα). The ratio of mercury and tin elements of the sample was analyzed by an Oxford Instruments INCA x-sight energy dispersive X-ray spectroscopy instrument with a JEOL TSM-6360 scanning electron microscope (SEM-EDX). The crystal structure was refined by the Rietveld method using the *RIETAN2000* program.[3] The X-ray data for Rietveld analysis were collected in the 2θ range from 20 to 120°, in the step interval of 0.02° at room temperature. The acquisition time was 2 s/step.

The diffuse reflectance spectrum was measured in the wavelength range 220−850 nm using a JASCO V-500 UV−VIS spectrophotometer.

The calculation of electronic structure was carried out using the full potential linearized augmented plane wave plus local orbital (FLAPW+lo) method with density functional theory (DFT), implemented in the software *WIEN2k*.[4,5] The generalized gradient approximation (GGA) based on the Perdew, Burke, and Ernzerhof scheme[6] was employed in this study for DFT. The final energy converged to 0.001 eV/atom.

(3) Izumi, F.; Ikeda, T. *Mater. Sci. Forum* **2000**, *198*, 321.
(4) Blaha, P.; Schwarz, K.; Madsen, G.; Kvasnicka, D.; Luitz, J. WIEN2k; An Augmented Plane Wave + Local Orbitals Program for Calculating Crystal Properties; Techn. Universität Wien: Austria, 2001 (ISBN3−9501031−1-2; http://www.wien2k.at/).

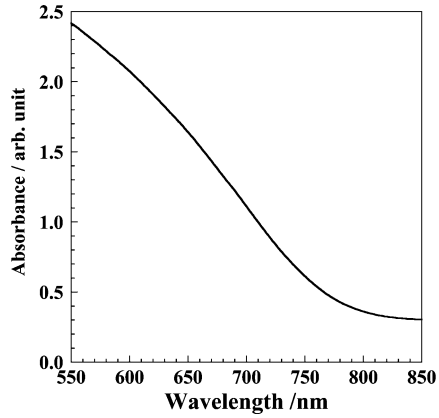

Figure 5. Absorbance spectrum of $HgSnO_3$.

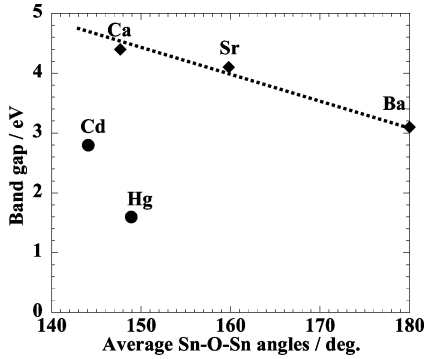

Figure 6. Optical band gap versus the Sn−O−Sn angle of $CaSnO_3$,[11] $SrSnO_3$,[11] $BaSnO_3$,[12] $CdSnO_3$,[2] and $HgSnO_3$.

Table 3. Parameters of the DOS Calculation for $HgSnO_3$ and $CaSnO_3$[a]

	R_{mt} (a.u.)	$R_{mt}k_{max}$	k point
$HgSnO_3$	Hg:1.99 Sn:1.73 O:1.73	7	489
$CaSnO_3$	Ca:2.15 Sn:1.90 O:1.90	7	144

[a] The structure parameters of $HgSnO_3$ and $CaSnO_3$ were taken from the final parameter of the Rietveld refinement and reference data.[11] The $R_{mt}K_{max}$ describes the plane wave cutoff parameter. The k point is the number of k points in the irreducible Brillouin zone (1000 k points in the whole Brillouin zone for $HgSnO_3$ and $CaSnO_3$).

The electronic resistivity of the sample was measured in the temperature range of 7 to 300 K by a conventional four-probe method using the sample with a rectangular parallel-piped arrangement.

The Seebeck coefficient of the sample was measured at temperatures ranging from 20 to 300 K. The temperature difference between verges of the sample was approximately 2 K.

The Hall coefficient measurement for the sample with a rectangular parallel-piped arrangement approximately 1.9 × 1.2 × 0.5 mm in size was carried out at 77 and 292 K. The magnetic field range was then 0 to 1 T, and the current was 2 mA.

3. Results and Discussion

3.1. High-Pressure Synthesis and Crystal Structure. We could not obtain a perovskite phase under 3 and 5 GPa. Figure 1 shows the XRD patterns for the samples synthesized under 7 GPa pressure at various temperatures. When the samples were synthesized using the stoichiometric mixture of HgO and SnO_2, the samples contained the trigonal-hexagonal phase, SnO_2, and unknown impurity phases at heating temperatures of 973 and 1073 K (parts (a) and (b) of Figure 1) and the trigonal-hexagonal phase with a small amount of SnO_2 at temperatures ranging from 1173 to 1373 K (parts (c)−(e) of Figure 1). Among these samples, though the least amount of SnO_2 was contained in the sample synthesized at 1273 K (part (d) of Figure 1), the single phase of $HgSnO_3$ was not obtained in these samples. According to the elemental analysis of the sample using the SEM-EDX, the average molar ratio of mercury to tin in the sample was 0.97 ± 0.01. Furthermore, we have confirmed from an elemental analysis using SEM-EDX that the gold capsule reacts with mercury. The reaction between the gold capsule and mercury produces a small amount of residual SnO_2, resulting in a ratio of mercury to tin of less than unity. When the sample was then synthesized using the HgO 5 mol% excess mixture at 1273 K (part (f) of Figure 1), a single trigonal-hexagonal phase was obtained. In this case, we confirmed that the average ratio of mercury to tin in the sample using SEM-EDX is 0.98 ± 0.02. Consequently, we obtained a single phase of $HgSnO_3$ with a mercury/tin ratio of unity by using the HgO 5% excess mixture under 7 GPa at 1273 K for 30 min. The sample synthesized under this condition was used for the crystal structure refinement and the measurement of the properties.

All of the X-ray diffraction peaks were indexed using a hexagonal unit cell. The reflection conditions derived from the indexed reflections of $HgSnO_3$ were $-h + k + l = 3n$ for hkl and $l = 6n$ for $00l$, affording possible space groups, non-centrosymmetric $R3c$ (No. 161) and centrosymmetric $R\bar{3}c$ (No. 167). Though the reliable factor of Rietveld refinement R_{wp} using $R3c$ (9.31%) is slightly smaller than that using $R\bar{3}c$ (9.72%) due to the larger number of parameters, the refined structural parameters such as fractional coordinates are very close, indicating that there is no apparent difference in the crystal structure. We therefore adopted centrocymmetric $R\bar{3}c$ with higher symmetry. The refined lattice parameters are $a = 0.5551(3)$ nm and $c = 1.3967(6)$ nm. Figure 2 shows the observed and calculated X-ray diffraction patterns. The refined structural parameters of $HgSnO_3$ are listed in Table 1. Here, the isotropic thermal parameter (B) of oxygen was fixed at 1.0 Å^2 because the value converges on a negative value. The selected metal−oxygen interatomic distances and the bond angle of $HgSnO_3$, calculated with ORFFE[7] are listed in Table 2. Figure 3 shows the refined crystal structure of $HgSnO_3$ from the perspective of the corner-shared SnO_6 octahedra framework. The antiphase tilting of the SnO_6 octahedron occurs around hexagonal [0001] (Glazer notation:[8] $a^-a^-a^-$) with a tilt angle of 19.69(5)°. According to Sleight and Prewitt[9] and Shan et

(5) Schwarz, K.; Blaha, P. *Comput. Mater. Sci.* **2003**, *28*, 259.
(6) Perdew, J. P.; Burke, S.; Ernzerhof, M. *Phys. Rev. Lett.* **1996**, *77*, 3865.
(7) Busing, W. R.; Martin, K. O.; Levy, H. A. *ORFFE, Report ORNL-TM-306*; Oak Ridge National Laboratory: TN, 1964.
(8) (a) Glazer, A. M. *Acta Crystallogr. Sect. B* **1972**, *28*, 3384. (b) Glazer, A. M. *Acta Crystallogr., Sect. A* **1975**, *31*, 756.
(9) Sleight, A. W.; Prewitt, C. T. J. *Solid State Chem.* **1973**, *6*, 509.

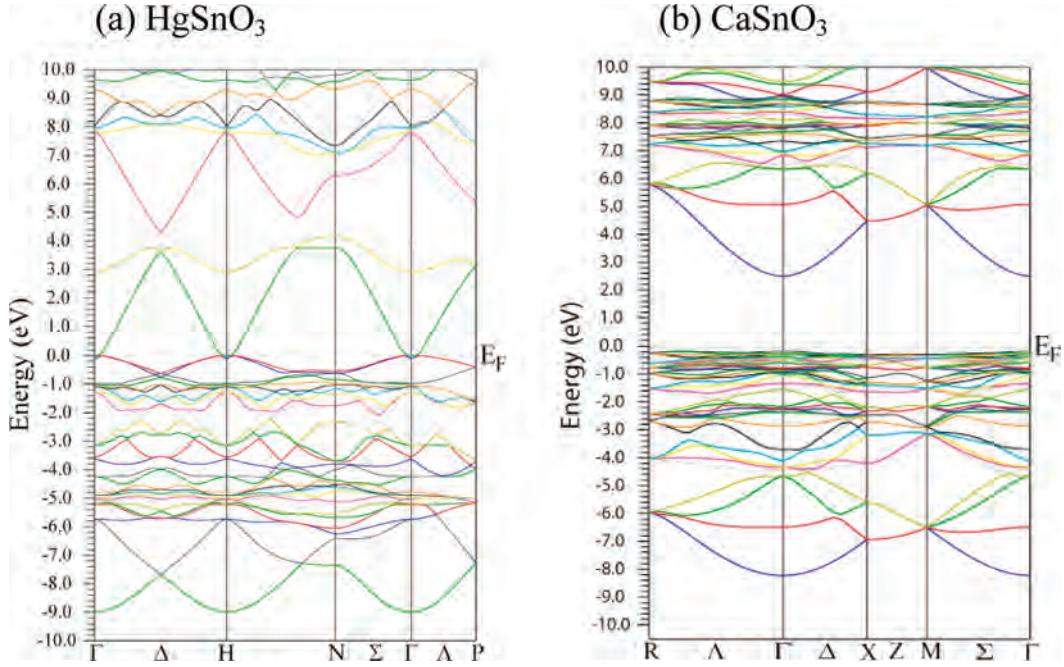

Figure 7. Calculated band structures of $HgSnO_3$ (a) and $CaSnO_3$ (b).

al.,[10] Hg-containing perovskites, $HgTiO_3$[9,10] and $HgPbO_3$,[9] also exhibit a rhombohedral distortion accompanied by the same type of antiphase octahedral tilting. In these compounds, the common characteristic is that mercury forms three short bonds to oxygen with distances of 2.2 Å.[9] The distortion is therefore attributed to the chemical bonding of mercury.

For comparison, the metal−oxygen interatomic distances and bond angles of $CaSnO_3$[11] are also listed in Table 2. Though the crystal symmetries for $HgSnO_3$ and $CaSnO_3$ are different ($HgSnO_3$ is rhombohedral ($R\bar{3}c$), and $CaSnO_3$ is orthorhombic (*Pnma*)), the Sn−O−Sn angles which represent the tilting level of the SnO_6 octahedron, and the average A−O distances are close. Thus, it is considered that the effect of the crystal structure on the electronic structure is similar between $CaSnO_3$ and $HgSnO_3$. $BaSnO_3$[11] possesses a cubic structure (ideal perovskite), whereas $SrSnO_3$,[11] $CaSnO_3$,[11] and $CdSnO_3$[2] possess an orthorhombic structure ($GdFeO_3$-type perovskite). Figure 4 shows the Sn−O−Sn angle versus the primitive cell volume for perovskite-type stannates $ASnO_3$ (A = Ba, Sr, Ca, Cd, Hg). The cell volume monotonously decreases with the decrease in the average Sn−O−Sn angle, indicating that the Sn−O−Sn angle is an important parameter that represents the structure of stannate perovskites.

3.2. Relationship between Crystal Structures and Optical Absorption in Stannnate Perovskites. The color of the $HgSnO_3$ powder sample is dark brown. To estimate the optical band gap, the diffuse reflectance spectrum was collected on the powder sample. The absorbance spectrum of $HgSnO_3$ at room temperatures is shown in Figure 5. Here, the diffuse reflectance data was transformed into absorbance with the Kubelka−Munk function. As a result, the band gap of $HgSnO_3$ was estimated to be 1.6 eV. Figure 6 shows the optical band gap versus the average Sn−O−Sn angle of $A'SnO_3$ (A′ = Ba, Sr, and Ca)[2] and $ASnO_3$ (A = Hg and Cd[2]). As seen in this figure, the band gap generally increases with decreases in the average Sn−O−Sn angle. This increase is due to the decrease in the conduction bandwidth in response to the increase in the SnO_6 octahedral tilting distortion. According to Mizoguchi et al.,[2] in $ASnO_3$ (A′ = Ba, Sr, and Ca), the top of the valence band is dominated by the contributions of the O 2p orbital, and the bottom of the conduction band is dominated by the contributions of the Sn 5s-O 2p interaction, and the decrease in the Sn−O−Sn angle from 180° induces a decrease in the interaction between Sn 5s and O 2p orbitals, resulting in a decrease in the conduction bandwidth and an increase in the band gap. Consequently, in $A'SnO_3$ (A′ = Ba, Sr, and Ca), the electronic structure in the vicinity of the Fermi level primarily arises from the interaction of tin and oxygen. Furthermore, when Figure 6 is examined in detail, it can be seen that the band gaps of $ASnO_3$ (A = Cd, and Hg) are smaller than those of $A'SnO_3$ (A′ = Ba, Sr, and Ca). This result implies that A-site ion also plays a role in the electronic structure of $ASnO_3$ (A = Cd, and Hg), as indicated by Mizoguchi et al.[2] This is likely to be the common characteristic of the A ions with the electron configuration $(n-1)d^{10}ns^0$; Cd^{2+}, $4d^{10}5s^0$ and Hg^{2+}, $5d^{10}6s^0$. We will discuss the contribution of mercury ion in $HgSnO_3$ to the electronic structure in the next section.

3.3. Electronic Structure of $HgSnO_3$. To understand the relationships between chemical bonding, crystal structure, and optical band gap, that is, the contribution of atomic orbitals to the electronic structure in the vicinity of the Fermi level, we carried out electronic structure calculations

(10) Shan, Y. J.; Inaguma, Y.; Tetsuka, H.; Nakamura, T.; Gaukler, L. J. *Ferroelectrics* **2006**, *337*, 71.
(11) Vegas, A.; Vallet-Regi, M.; González-Calbet, J. M.; Alario-Franco, M. A. *Acta Crystallogr. Sect. B* **1986**, *42*, 167.

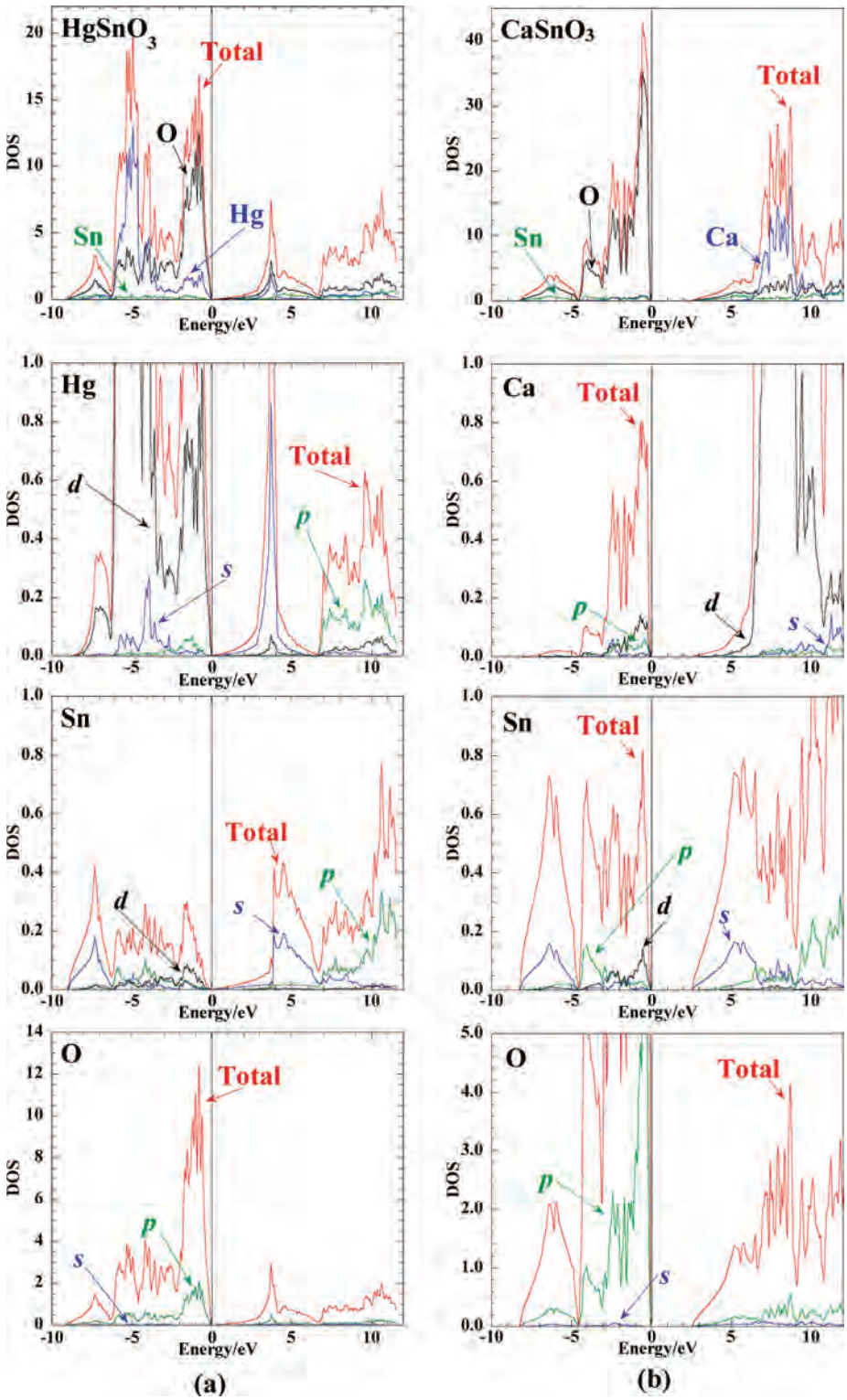

Figure 8. Calculated density of the state of $HgSnO_3$ (a) and $CaSnO_3$ (b). The Fermi level is at 0 eV.

for $HgSnO_3$ in comparison with $CaSnO_3$. We used the reported crystal structure data of $CaSnO_3$[11] for the calculation. Table 3 shows the parameters for the calculations. Figures 7 and 8 show the calculated electronic band structure and the total density of states (DOS) along with the Hg-s/-p/-d, Ca-s/-p/-d, Sn-s/-p/-d, and O-s/-p partial DOS for $HgSnO_3$ and $CaSnO_3$. In the case of $CaSnO_3$, the valence band maximum is located at the Γ point, and the conduction band minimum is located at the Γ point, resulting in a direct energy band gap of 2.4 eV. This result is approximately consistent with the reported calculation value (2.9 eV),[2] which shows the validity of our calculation. In contrast, in the case of $HgSnO_3$, there is no energy band gap, indicating that $HgSnO_3$ is metallic. The band gap of $HgSnO_3$ is, however, estimated to be 1.6 eV by the result of optical absorbance as indicated above. We

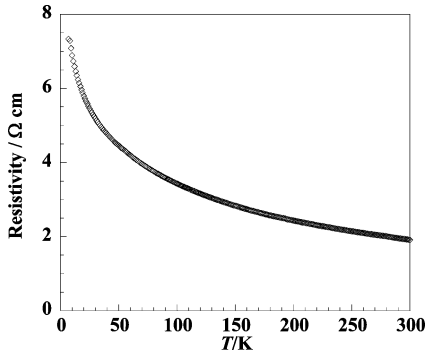

Figure 9. Temperature dependence of electrical resistivity for as-synthesized $HgSnO_3$.

note that because of the approximate nature of DFT calculation with GGA, the theoretically calculated band gaps are inaccurate and somewhat smaller than the experimental values. It has also been reported that the calculated band gaps of $ASnO_3$ (A = Ba, Sr, Ca, Cd) are smaller than the experimental values[2] by 1−2 eV as well as those of $HgSnO_3$. Though we failed to accurately reproduce the experimental band gap, the contribution of each orbital to the electronic structure in $HgSnO_3$ can be derived from the calculation. We can therefore discuss the contribution of valence and conduction band in $HgSnO_3$. In the case of $CaSnO_3$, the top of the valence band and the bottom of the conduction band are dominated by the O 2p orbital and the Sn 5s-O 2p interaction, respectively, and no contributions of the Ca 4s orbital to either the conduction or the valence bands were observed. This characteristic of electronic structure is observed in other alkaline stannates, $BaSnO_3$ and $SrSnO_3$. Therefore, the band gap in alkaline stannates primarily depends on the tilt angle of the SnO_6 octahedron. In contrast, in the case of $HgSnO_3$, the effect of the orbital of mercury on the electronic structure cannot be ignored. As shown in Figure 8, the band at 0.0−3.8 eV is dominated by the orbitals of Hg 6s, Sn 5s, and O 2p, whereas the band at −0.7 to 0.0 eV is dominated by orbitals of Hg 5d, Sn 4d, and O 2p. For $HgSnO_3$, the width of the conduction band is increased by the contribution of the Hg 6s orbital to Sn 5s − O 2p, and the width of valence band is increased by the contribution of the Hg 5d orbital to O 2p. Hence, the band gap of $HgSnO_3$ narrows in comparison with that of $CaSnO_3$ due to the participation of the Hg 5d and 6s orbital in bonding in the vicinity of the Fermi level, even though the tilt angle of the SnO_6 octahedron is close to that of $CaSnO_3$.

3.4. Transport Properties of As-Synthesized $HgSnO_3$. The large dispersion of the conduction band of $HgSnO_3$ seen in part (a) of Figure 8 suggests that n-doped $HgSnO_3$ should possess a relatively large mobility. We therefore evaluated the transport properties of $HgSnO_3$. As-synthesized $HgSnO_3$ exhibited the low resistivity of 2 Ωcm at 300 K. Figure 9 shows the temperature dependence of the electronic resistivity of as-synthesized $HgSnO_3$. The resistivity, ρ, slightly increases with decreases in the temperature. The Hall coefficient, R_H, is negative throughout the measured temperature range, indicating that the carrier is the electron. The Hall coefficient, R_H, the carrier concentration, n, and the Hall mobility, μ, at 77 and 292 K are listed in Table 4. Here, we estimate the carrier concentration and Hall mobility using the following eqs 1 and 2.

Table 4. Results of the Hall Coefficient and the Carrier Density of $HgSnO_3$

	Hall coefficient, $cm^3 \cdot C^{-1}$	carrier density, cm^{-3}	Hall mobility, $cm^2 \cdot V^{-1} \cdot s^{-1}$
292 K	−13.0(10)	$4.8(4) \times 10^{17}$	6.7(5)
77 K	−21.0(3)	$2.97(4) \times 10^{17}$	5.5(8)

$$R_H = -\frac{1}{ne} \quad (1)$$

$$\rho = \frac{1}{\sigma} = \frac{1}{ne\mu} \quad (2)$$

The estimated carrier concentration at 77 K is slightly smaller than that at 292 K. The carrier concentration is on the order of 10^{17} cm^3, corresponding to the order of 10^{-5} electrons per unit cell at 292 K. The small carrier concentration can be attributed to a trace of impurity phase or oxygen defects. The small temperature dependences of the resistivity and the carrier concentration indicate that the donor level due to cation substitution of impurity level or oxygen vacancy is formed below the conduction band and that the electrons are easily excited to the conduction band. The Hall mobility is 6.7(5) cm^2 V^{-1} s^{-1} at 292 K, which is comparable to the mobilities of other oxide semiconductors, including main group cations, which range from 1 to 100 cm^2 V^{-1} s^{-1}. This finding accords with the calculated conduction band with large dispersion. Figure 10 shows the temperature dependence of the Seebeck coefficient of as-synthesized $HgSnO_3$. The Seebeck coefficient is negative in the whole temperature range and decreases linearly with temperature. The negative value indicates that the carrier of as-synthesized $HgSnO_3$ is the electron, which is consistent with the results of the Hall coefficient measurement. A linear temperature dependence for the Seeback coefficient is often observed for metallic conductors. The metallic-like temperature dependence of the Seebeck coefficient in as-synthesized $HgSnO_3$ is probably due to the small temperature dependence of carrier concentration, which in turn is due to the small energy difference between the donor level and the conduction band edge.

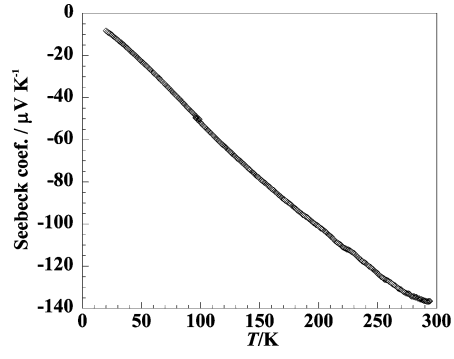

Figure 10. Temperature dependence of the Seebeck coefficient for as-synthesized $HgSnO_3$.

4. Conclusion

We synthesized a new perovskite-type oxide, $HgSnO_3$, under high pressure and high temperature and investigated its crystal and electronic structures as well as transport properties. We obtained a single phase of $HgSnO_3$ under 7 GPa at 1273 K for 30 min. The $HgSnO_3$ was found to form a trigonal-hexagonal unit cell with the space group $R\bar{3}c$. The perovskite $HgSnO_3$ exhibits rhombohedral distortion with the antiphase tilting of SnO_6 octahedra around [0001] ([111] for perovskite sub cell). The electronic structure in the vicinity of the Fermi level of $HgSnO_3$ was found to be strongly influenced by the participation of the orbital of mercury, that is, the widths of the conduction and valence bands are increased by the contribution of Hg 6s and Hg 5d orbitals, respectively. As-synthesized $HgSnO_3$ is an n-type semiconductor according to the results of the resistivity, Seebeck coefficient, and Hall coefficient measurements.

Acknowledgment. The authors thank Dr. Ko-ichi Hiraki, Dr. Ryo Chiba, and Prof. Toshihiro Takahashi of Gakushuin University for their help with the Hall coefficient measurement and Dr. Hiroyuki Tetsuka and Prof. Yue-Jin Shan of Utsunomiya University for their help with the electronic structure calculations. This work was supported by the "High-Technology Research Center Project" of the Ministry of Education, Culture, Sports, Science, and Technology of Japan.

IC800370R

(12) Smith, A. J.; Welch, A. J. E. *Acta Crystallogr.* **1960**, *13*, 653.